6-2015

Difference equation for tracking perturbations in systems of Boolean nested canalyzing functions

Elena S. Dimitrova
Clemson University

Oleg I. Yordanov
Bulgarian Academy of Sciences

Mihaela Teodora Matache
University of Nebraska at Omaha, dvelcsov@unomaha.edu

A DIFFERENCE EQUATION FOR TRACKING PERTURBATIONS IN SYSTEMS OF BOOLEAN NESTED CANALYZING FUNCTIONS

ELENA S. DIMITROVA[+], OLEG I. YORDANOV[◇], MIHAELA T. MATACHE[†*]

[+]Mathematical Sciences, Clemson University, Martin O-303
Clemson, SC 29634-0975, USA
edimit@clemson.edu

[◇]Institute of Electronics, Bulgarian Academy of Sciences (BAS)
72 Tsarigradsko Chaussee, 1784 Sofia, Bulgaria
oleg.yordanov@gmail.com

[†]Department of Mathematics, University of Nebraska at Omaha
Omaha, NE 68182, USA
dmatache@unomaha.edu

[*]corresponding author

Abstract. The article studies the spread of perturbations through networks composed of Boolean functions with special canalyzing properties. Canalyzing functions have the property that at least for one value of one of the inputs the output is fixed, irrespective of the values of the other inputs. In this paper the focus is on partially nested canalyzing functions, in which multiple, but not all inputs have this property in a cascading fashion. They naturally describe many relationships in real networks. For example, in a gene regulatory network, the statement "if gene A is expressed, then gene B is not expressed regardless of the states of other genes" implies that A is canalyzing. On the other hand, the additional statement "if gene A is not expressed, and gene C is expressed, then gene B is automatically expressed; otherwise gene B's state is determined by some other type of rule" implies that gene B is expressed by a partially nested canalyzing function with more than two variables, but with two canalizing variables. In this paper a difference equation model of the probability that a network node's value is affected by an initial perturbation over time is developed, analyzed, and validated numerically. It is shown that the effect of a perturbation decreases towards zero over time if the Boolean functions are canalyzing in sufficiently many variables. The maximum dynamical impact of a perturbation is shown to be comparable to the average impact for a wide range of values of the average sensitivity of the network. Percolation limits are also explored; these are parameter values which generate a transition of the expected perturbation effect to zero as other parameters are varied, so that the initial perturbation does not scale up with the parameters once the percolation limits are reached.

Keywords: partially nested canalyzing functions, Boolean network, perturbation, dynamical impact, expected damage, sensitivity

1. Introduction

A large influx of biological data on the cellular level has necessitated the development of innovative techniques for modeling the underlying networks that regulate cell activities. Several discrete approaches have been proposed, such as Boolean networks [1], logical models [2], and Petri nets [3]. In particular, Boolean networks have emerged as popular models for gene regulatory networks [4, 5]. However, not all Boolean functions accurately reflect the behavior of biological systems, and it is imperative to recognize classes of functions with biologically relevant properties.

One such notable class is the canalyzing functions, introduced by Kauffman [6] as appropriate rules in Boolean network models of gene regulatory networks since their behavior mirrors biological properties described by Waddington [7]. Canalyzing functions naturally describe many relationships in a gene regulatory network. For example, the statement "if gene A is expressed, then gene B is not expressed regardless of the states of other genes" implies that A is canalyzing. The dynamics of Boolean networks constructed using these functions are of great interest when determining their modeling potential [8, 9]. For instance, Karlssona and Hörnquist [8] explore the relationship between the proportion of canalyzing functions and network dynamics. Random Boolean networks constructed using such functions have been found to be more stable than networks of general Boolean functions, in the sense that they are insensitive to slight perturbations [9].

In [9], the authors further expand the canalyzing concept and introduce the class of nested canalyzing functions (NCFs). For instance, in [10], networks of NCF's were shown the exhibit stable dynamics. Also, Nikolajewa, *et al.* [11] divide NCF's into equivalence classes based on their representation and show how the network dynamics are influenced by choice of equivalence class.

However, NCFs are very restrictive in structure as noted in Layne, *et al.* [12], since some nodes may not exhibit the canalyzing behavior at all. The authors of [12] consider functions that have a partially nested canalyzing structure rather than a fully nested canalyzing structure, defining the nested canalyzing depth as the degree to which a function exhibits a canalyzing structure in comparison to its number of inputs. The results in [12] were expanded by Jansen and Matache [13], taking into account the states composing the limiting cycles of networks composed of such partially nested canalyzing functions (PNCFs).

The spread or propagation of a local perturbation has been studied in the literature under various network scenarios mostly by considering the average sensitivity of the individual functions or the entire network. Examples include random Boolean networks or versions of them evolved for high dynamical robustness [14], random threshold networks [15], networks governed by distributions of functions found from biological data [16], or

more recently on networks governed by veto functions for which the output is shut off by a single inhibitory signal regardless of other inputs [17].

The paper is structured as follows. In Section 2 we introduce the Boolean networks under consideration governed by PNCFs and construct the mathematical model for tracking perturbations along the trajectories of the network and assessing the probability that a node is affected by a small perturbation after a given number of iterations of the network. In Section 3 we validate the model by a direct comparison to perturbation results obtained from an actual PNCF network with similar parameters, followed by a theoretical analysis of the steady states of the map generated by the tracking model. The analysis of that map is continued in Section 4 where the map is viewed as the dynamical impact of an initial perturbation perturbation after k time steps in relation to the average sensitivity of the network. We continue with a study of the percolation transitions with respect to the network size, and the canalyzation depth viewed also as a fraction of the number of variables of the PNCFs. The results provide a further in-depth understanding of the long term effect of perturbations on a PNCF network. We end with a discussion and further directions of research in Section 5.

2. Tracking perturbations in partially nested canalyzing functions

2.1. **Nested canalyzing functions.**

We first review the concept of canalyzing functions in general, after which we focus on nested canalyzation. Denote $\mathbb{B} = \{0, 1\}$.

Definition 1. *A Boolean function $f(x) = f(x_1, \ldots, x_n)$ is* canalyzing *if it has a variable x_i for which a particular input $x_i = a_i$ implies that $f(x) = b_i$ for some $b_i \in \mathbb{B}$. In this case, x_i is called a* canalyzing variable*, the input a_i is its* canalyzing value*, and the output value b_i when $x_i = a_i$ is the corresponding* canalyzed value*. Note that if f is constant, then every variable is trivially canalyzing.*

If a canalyzing variable x_i does not receive its canalyzing input a_i, then the output of the function f is determined by a function $g(\hat{x}_i)$, where $\hat{x}_i = (x_1, \ldots, x_{i-1}, x_{i+1}, \ldots, x_n)$. If this function g is constant, x_i is called a *terminal canalyzing variable* of f. Note that for each $i \neq j$, x_j is then trivially canalyzing in g.

If g is not constant, it is natural to ask whether it too is canalyzing. If so, then there is a canalyzing variable x_j with canalyzing input a_j, and when $x_j \neq a_j$, the output of f is a function $g(\hat{x}_{ij})$, which may or may not be canalyzing. Here, $\hat{x}_{ij}$ denotes x with both x_i and x_j omitted. Eventually, this process will terminate when the function g is either constant or no longer canalyzing. The formal definition follows.

Definition 2. *Let $f(x_1, \ldots, x_n)$ be a Boolean function. Suppose that for a permutation σ of the numbers $1, 2, \ldots, n$, some $d \in \{1, 2, \ldots, n\}$, and a Boolean function $g(x_{\sigma(d+1)}, \ldots, x_{\sigma(n)})$,*

$$f = \begin{cases} b_1 & x_{\sigma(1)} = a_1 \\ b_2 & x_{\sigma(1)} \neq a_1,\ x_{\sigma(2)} = a_2 \\ b_3 & x_{\sigma(1)} \neq a_1,\ x_{\sigma(2)} \neq a_2,\ x_{\sigma(3)} = a_3 \\ \vdots & \vdots \\ b_d & x_{\sigma(1)} \neq a_1, \ldots,\ x_{\sigma(d-1)} \neq a_{d-1},\ x_{\sigma(d)} = a_d \\ g & x_{\sigma(1)} \neq a_1, \ldots,\ x_{\sigma(d)} \neq a_d \end{cases} \tag{1}$$

where either b_d is a terminal canalyzing variable (and hence g is constant), or g is non-constant and none of the variables $x_{\sigma(d+1)}, \ldots, x_{\sigma(n)}$ are canalyzing in g. Then f is said to be a partially nested canalyzing function *(PNCF). The integer d is called the* active canalyzing depth *of f, and the (full) nested canalyzing* depth *of f is d if g is non-constant, and n otherwise. The sequence $x_{\sigma(1)}, \ldots, x_{\sigma(n)}$ is called a* canalyzing sequence *for f.*

The class of *nested canalyzing functions* (NCFs) [18, 9] are precisely those with active depth n. In [12] it is shown that the average sensitivity of a Boolean network to small perturbations of a PNCF increases as the canalyzing depth increases; however the difference in sensitivity between PNCFs of sufficient depth and NCFs is very slight. Additionally, it is shown that the dynamics of networks with PNCFs rapidly approach the critical regime, whereas networks with functions of relatively few nested canalyzing variables can remain in the chaotic phase as was found in [19]. In [12], the average sensitivity is computed assuming ergodicity of the network, that is all inputs can arise with the same probability during evolution, and the time average over the states visited by the network yields the same result as the average over the whole phase space. Later, in [13], the authors extend the work of [12] to non-ergodic networks by taking into account the states composing

the limiting cycles of PNCF networks, and find the average sensitivity to minimal initial perturbations, and the corresponding phase transitions using a complementary threshold function g in the definition of PNCFs. The average sensitivity is used to identify the critical curve that separates order from chaos.

In this paper, we take matters one step further by tracking the actual perturbations along the trajectories of the network and assess the probability that a node is affected by a small perturbation after a given number of iterations of the network. This model is described next.

2.2. **Tracking perturbations.** For simplicity we will consider the case when the canalyzing variable order is $x_1, \ldots, x_n$ for all functions $f_i, i = 1, 2, \ldots, n$ in the network. The actual connectivity of the nodes may be smaller than the total number of nodes. We assume a common canalyzation depth d for all nodes, with $d = n$ for NCFs.

Let $\mathbf{x_0}$ be an initial state of the system and $[\mathbf{x_0}]_i$ be its ith bit. Suppose that with no perturbation, $F(\mathbf{x_0}) = \mathbf{x_1}$, where $F = (f_1, f_2, \ldots, f_n)$. Let $\mathbf{y} \in \mathbb{B}^n$ be a perturbation. We are interested in the probability that $[\mathbf{x_1}]_i$ is different from $f_i(\mathbf{x_0} \oplus \mathbf{y})$, where $\oplus$ is the XOR operator. That is, we want to determine $\Pr[f_i(\mathbf{x_0}) \neq f_i(\mathbf{x_0} \oplus \mathbf{y})]$.

Let $m = \min\{j \in \{1, \ldots, n\} \mid [\mathbf{y}]_j = 1\}$, *i.e.* m is the index of the most "influential" variable that is perturbed. Since variable x_m has impact on the function's output only if the first $m - 1$ variables did not assume their canalyzing values,

$$y_0 = \Pr[f_i(\mathbf{x_0}) \neq f_i(\mathbf{x_0} \oplus \mathbf{y})] = \frac{1}{2^m} \cdot \left(1 - \frac{1}{2^d}\right) + \frac{1}{2^{d+1}} \cdot \left(\frac{1}{2^d} - \frac{1}{2^n}\right). \tag{2}$$

This can be extended for any number of updates of the system. Let k be the number of times the system was updated starting at $\mathbf{x_0}$. Then $\mathbf{x_k}$ is the state of the system after k updates and let $\mathbf{x'_k}$ be the system's state when the system's initial state was perturbed, that is, the initial state was $\mathbf{x_0} \oplus \mathbf{y}$ instead of $\mathbf{x_0}$. Let $y_k = \Pr[[\mathbf{x'_k}]_i \neq [\mathbf{x_k}]_i]$. Assuming that no more perturbations were applied, the probability that a perturbation is still affecting the ith bit after $k + 1$ iterations is given by the following difference equation:

$$y_{k+1} = \sum_{j=1}^{d} (1 - y_k)^{j-1} y_k \frac{1}{2^j} + \sum_{j=d+1}^{n} (1 - y_k)^{j-1} y_k \frac{1}{2^{d+1}}$$

$$= \frac{(1 - \frac{1}{2^d}(1 - y_k)^d)y_k}{1 + y_k} + \frac{(1 - y_k)^d - (1 - y_k)^n}{2^{d+1}} \tag{3}$$

with initial condition (2). Notice that the effect of a particular perturbation depends only on the position of the most influential variable that is perturbed. The first sum in (3) is for the case when the most influential variable j that is perturbed is one of the d canalyzing variables, while the second sum corresponds to the remaining $n - d$ non-canalyzing variables. Then the first $j-1$ variables have to be unchanged with probability $1-y_k$ each. This leads to the powers of $1-y_k$ in (3) by assuming independence. We point out that the main assumptions for the equation (3) are: a uniform distribution of inputs, that is we assume an ergodic network; the probability that an input is on its canalyzing value, the probability that a canalyzing input is an activator, and the probability that a canalyzed output value is 1 are all equal to 1/2. Also, the function g that takes over if the canalyzing inputs are not on their canalyzing values is biased with bias 1/2; thus the probability of an output 1 is equal to 1/2 when applying g. These assumptions explain the powers of 1/2 in (3), since the first $j-1$ inputs cannot be on their canalyzing values, and the jth one has to produce a change in the output. Notice that we only apply a perturbation at the initial state. In a real situation, perturbations are possible at any stage of the network evolution. While the mathematical framework is very similar, here we consider the basic case that lends itself to presentation and analysis and leave the more general case for future work.

The difference equation (3) has interesting properties. Independent of the values of n and d, it has a fixed point at zero, $y_0^\star = 0$. Let $y_{k+1} = f(y_k)$. Notice that $f_{max} = f(1) = 1/2$, so the solutions are bounded above by 1/2. Note also the weak dependence on n: unless y_k is very small, the term that involves n is of order $1/2^{d+n+1}$. Calculating the derivative of $f(y)$ at zero we obtain:

$$f'(0) = 1 + \frac{n - d - 2}{2^{d+1}}, \tag{4}$$

which is less than or equal to one for $n \leq d + 2$. Hence, for $d \leq n \leq d + 2$ the graphs of $f(y)$ are below the diagonal and for an arbitrary initial condition the solutions, albeit

very slowly, decrease to zero. However, for $n > d + 2$, $y_0^\star$ becomes repellent and there occurs a second fixed point $y^\star > 0$, an exact solution of which is not so easy to find and an approximation is needed. Assuming that $y^\star$ is small an approximation can be constructed by just taking the first two terms of the Taylor expansion of $f(y_k)$ at zero. This leads to

$$y^\star \approx 2\frac{1 - f'(0)}{f''(0)}, \tag{5}$$

and after substituting the expressions for the derivatives,

$$y^\star \approx \frac{2(n - d - 2)}{2^{d+2} + [n(n-1) - d(d-1) - 4(d+1)]}. \tag{6}$$

Thus, we realize that the effect of a perturbation decreases towards zero over time if a system consists of nested or "almost" nested canalyzing functions, *i.e.* when the function depth is $d \geq n - 2$, which is consistent with what we expect from such systems. When $d < n - 2$, the perturbation does not die out. For $y_0 > y^\star$ the perturbation decreases over time, while for $y_0 < y^\star$ it increases. In both cases it converges to $y^\star$, whose value according to (6), however, is small. A more accurate approximation will be obtained in the next section.

2.3. **State space structure of systems of NCFs.** We can also think of $\mathbf{x_0} \oplus \mathbf{y}$ as another vertex in the state space graph of the system. Consider (3) in this context. Let $\mathbf{x_0}$ and $\mathbf{x'_0}$ be two different vertices of the systems (two initial states) and let m be the smallest index such that $[\mathbf{x'_0}]_m \neq [\mathbf{x_0}]_m$. If $\mathbf{x_t}$ and $\mathbf{x'_t}$ is the state of the system after t updates when starting at $\mathbf{x_0}$ and $\mathbf{x'_0}$, respectively, then (3) gives the probability that starting from the two different states, the system does not converge to the same state after t steps. Since this probability is very small for systems composed of NCFs or PNCFs of sufficient depth, we can expect that on average the state spaces of such systems systems have short trajectories, small cycles, and a small number of components. Numerical simulations confirm that [20]. Notice that here we assumed that all local functions have the same canalyzing variable order. The generalization for different orders is straightforward.

3. Validation of the tracking model and analysis of steady states

The numerical approaches encompass the validation of the model by a direct comparison to perturbation results obtained from an actual PNCF network with similar parameters, followed by a theoretical analysis of the steady states of the map (3).

3.1. **Validation.** In order to validate the model for y_k, the probability that a perturbation is still affecting the ith bit after k iterations, we compare the model with the normalized Hamming distance obtained from a network with identical parameters as the model. More precisely, we generate an actual PNCF network and select an initial condition $\mathbf{x_0}$ randomly. Then we apply an initial perturbation $\mathbf{y}$ to obtain a second initial condition given by $\mathbf{x'_0} = \mathbf{x_0} \oplus \mathbf{y}$. We update the network k steps to obtain $\mathbf{x_k}, \mathbf{x'_k}$. Then we compute $H_k = \frac{1}{n} \sum_{i=1}^{n} ([\mathbf{x_k}]_i \oplus [\mathbf{x'_k}]_i)$ representing the normalized Hamming distance between the two states of the network. We average both H_k and y_k over different initial conditions, and plot them versus k to assess the accuracy of the estimation given by y_k. We also plot the corresponding Derrida plots of H_{k+1} versus H_k. A few results are shown in Figure 1 for a networks with $n = 64$ nodes, canalyzing depth $d = 1, 2, 5$, and initial perturbation of 8 nodes. These plots represent a small sample of the numerical simulations performed in Matlab to validate the model. We note that the model is fairly close to the network results, and the Derrida plots are located mostly along the main diagonal, indicating a complex behavior of the dynamics. So the model is a good fit for the effect of perturbations on a PNCF network, and we can use it for further explorations.

3.2. **Analysis of steady states.** We are now analyzing further the map $y_{k+1} = f(y_k)$ given by (3). As noted before, the function has at least one fixed point at $y_0^\star = 0$. In order to search for other fixed points, if they exist, and at the same time to illustrate the iterations of $f(y_k)$, we plot graphs of f in the interval $[0, 1]$ for $d = 10$ and six values of the parameter n. This is done in Figure 2. We show a cobweb plot of an initial condition as well.

On this scale the graphs of $f(y_k)$ are practically indistinguishable. We saw that $f'(0) \leq 1$ for $n \leq d + 2$. Hence, for $d \leq n \leq d + 2$ the graphs of $f(y_k)$ are below the diagonal and the solutions independent of the initial y_0 decrease to zero. On the other hand, for

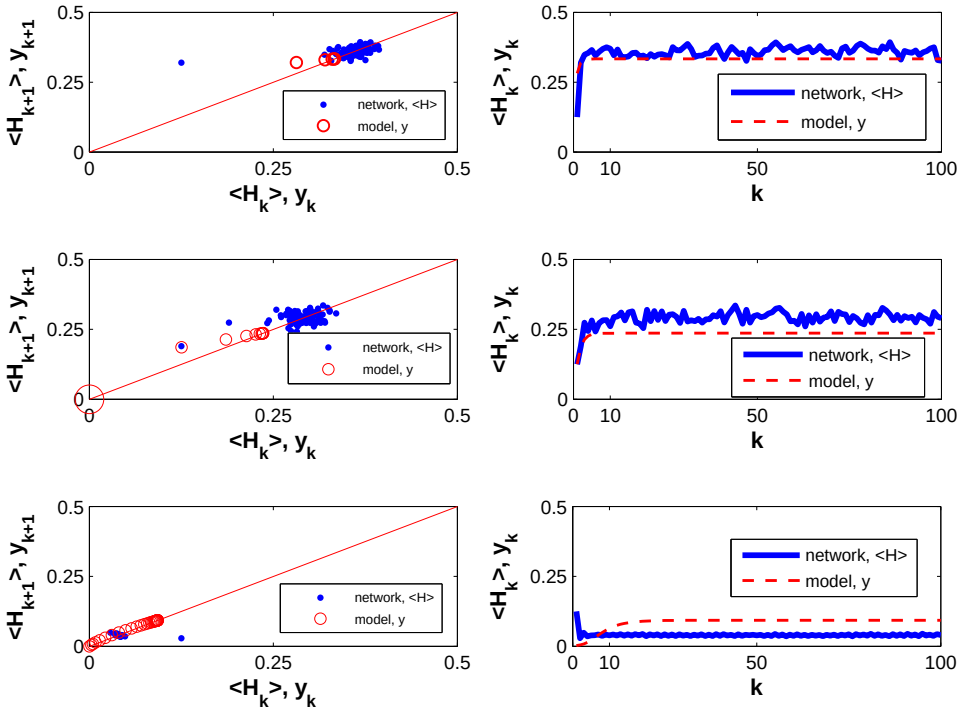

FIGURE 1. (Color online) Hamming distance versus model (left column), for PNCF network with $n = 64, d = 1$ (first row), $d = 2$ (second row), and $d = 5$ (third row). The Hamming distance is computed over a number of random initial conditions. Both the network and the model are iterated 100 steps, and the actual corresponding values are plotted in the right column. The initial perturbation is on 8 randomly selected nodes. Notice that although there is not a perfect match (due also to rounding errors on small numbers), the model follows pretty closely the network results.

$n > d + 2$, the fixed point at zero becomes repellent and although not seen on the scale of the graph, there must be at least a second fixed point $y^\star > 0$. However, this point cannot be discerned even on scale of the graph of 0.025×0.025 (not shown). To clarify their positions graphically we plot $f(y_k) - y_k$ against y_k in Figure 3, where the locations of the fixed points are indicated by the intersections of the curves not with the diagonal but with the horizontal axis. A trajectory with initial value $y_0 \geq y^\star$ will decrease toward $y^\star$; those with $0 < y_0 < y^\star$ will be increasing, slowly converging to $y^\star$.

Next, we approximate the position of the second fixed point by taking $\varepsilon = 1/2^{d+1}$ as a small parameter in the equation $f(y) - y = 0$. Multiplying through by $(1 - y_k)$, changing variables $y_k = 1 - z_k$, factoring out $(1 - z_k)$ (the factor corresponding to the fixed point

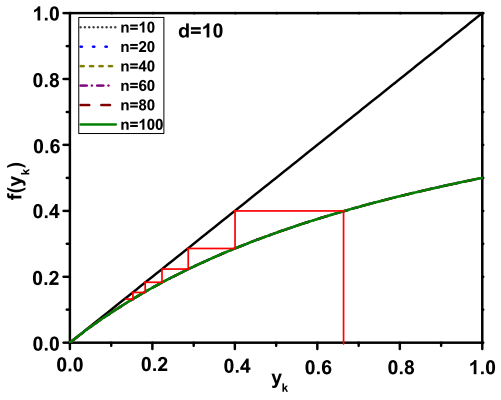

FIGURE 2. (Color online) Graphs of the function $f(y_k)$ given by (3) for $d = 10$ and six values of parameter n (see legend). Observe that the graphs are practically superimposed. The red ladder illustrates graphically the first few iterations of (3), generating a cobweb plot.

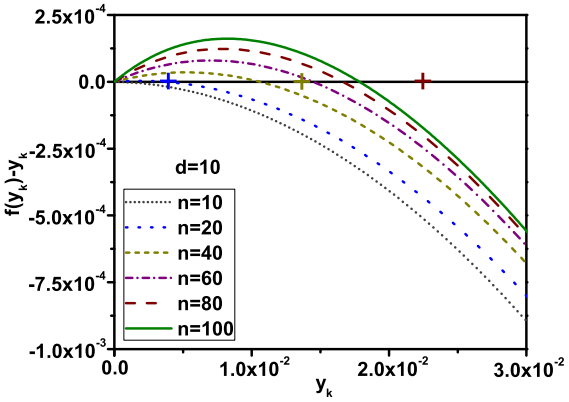

FIGURE 3. (Color online) Graphs of the function $f(y_k) - y_k$ for $d = 10$ and six values of parameter n (see legend). The points at which the graphs cross the horizontal axis represent the second fixed points of the map (3).The crosses indicate the leading order approximation,(8), for $n = 20, 40$, and 60 (left to right).

at zero), and re-scaling by substituting $z_k = \varepsilon^{-1/(n-1)}u$, we obtain

$$u^n - u = \varepsilon_s u^{n-1} + \varepsilon_s^2 u^{n-2} + \cdots + \varepsilon_s^{n-d-2} u^{d+2} - \varepsilon_s, \tag{7}$$

where $\varepsilon_s = \varepsilon^{1/(n-1)}$ was introduced to denote the effective small parameter for the re-scaled equation. (Through the re-scaling, we have eliminated the small parameter at the highest degree term.) If we set $\varepsilon_s = 0$, equation (7) has two real roots, $u = 0$ and $u = 1$.

Of these, $u = 0$ leads to the approximation of the fixed point in the unit interval. Thus, we look for a solution in the form of the series $u^\star = \varepsilon_s \left(u_1^\star + u_2^\star \varepsilon_s + u_3^\star \varepsilon_s^2 + \cdots\right)$. It is immediately inferred that $u_1^\star = 1$ and $u_i^\star = 0$ for all $i = 2, 3, \ldots (n-1)$. The next term yields $u_n^\star = -(n-d-2)$, which upon returning to the original variables results in the following leading order approximation:

$$y^\star \approx \frac{(n-d-2)}{2^{d+1}}. \tag{8}$$

This approximation for cases corresponding to $n = 20, 40$, and 60 is shown in Figure 3 by the crosses. Clearly, the approximate values overestimate the true ones by an error which increases with n; for the cases $n = 80$ and $n = 100$, the values of $y^\star$ are outside of the picture's scale; $y^\star \approx 0.033$ and $y^\star \approx 0.043$, respectively.

To improve the approximation, we sum a subseries of $u^\star$, which includes all terms having the form $u^\star_{i(n-1)+1}$, $i = 0, 1, 2, \ldots$, neglecting the contribution of the cross-product terms. It is straightforward to infer $u^\star_{i(n-1)+1} = u_n^\star b^{i-1}$, where $b = -\left(n(n-3) - d(d+1)\right)/2$. Summing the subseries and going back to the variable y_k results in

$$y^\star \approx \frac{2(n-d-2)}{2^{d+2} + (n(n-3) - d(d+1))}. \tag{9}$$

This expression is similar to (6), but it is a more accurate approximation. To illustrate the accuracy of (9), we compare it with the numerical evaluation of the fixed point, see Table 1. The error compared to that of (8) is reduced, however, now the approximate values systematically underestimate the numerical solution. The bias is likely due to the neglected cross-product terms.

The second fixed point is always attractive. This follows from the fact that $f(y_k)$ has no maximum on the unit interval. Also, since $f'(1) = 1/4$, the derivative of the map is positive on the entire interval and therefore the iterations converge to $y^\star$ monotonically. The convergence is slow and gets slower for large values of n in comparison to d. In Figure 4 we show the Lyapunov exponents calculated at 0.4 (any other initial value yields the same results) and the bifurcation diagrams along d for two fixed values of n, which further illustrates the properties of the map. Except for small d, the values of the Lyapunov

d	n	$y^\star$–numerical	$y^\star$–approximate
10.0	20.0	3.7035×10^{-3}	3.6986×10^{-3}
10.0	40.0	1.0578×10^{-2}	1.0245×10^{-2}
10.0	60.0	1.4469×10^{-2}	1.2962×10^{-2}
10.0	80.0	1.6619×10^{-2}	1.3404×10^{-2}
10.0	100.0	1.7845×10^{-2}	1.2860×10^{-2}

TABLE 1. Comparison of the numerical and the approximate values of $y^\star$ for a fixed value of d and various values of n. Notice that the numerical value is always greater than the approximate value.

exponents are close to zero, but negative. The bifurcation diagrams is basically comprised of the two fixed points, $y_0^\star = 0$ and $y^\star$, and shows the second point converging to zero.

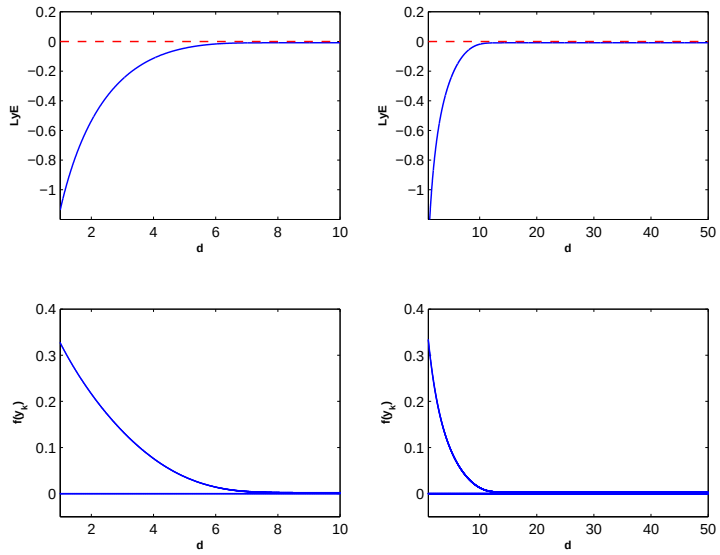

FIGURE 4. (Color online) Top panels: Lyapunov exponents for $f(y_k)$ as functions of the canalyzing depth d. Bottom panels: bifurcation diagrams for the same values of the parameters. The left panels correspond to $n = 10$, while the right panels correspond to $n = 50$.

Thus, in this section we have validated the model and analyzed the steady states of the model. We can further use it to assess the impact of perturbations on a PNCF network.

4. Dynamical impact of perturbations and expected damage

In this section we present an analysis of the map (3) viewed as the dynamical impact of an initial perturbation after k time steps in relation to the average sensitivity of the network. We continue with a study of the percolation transitions with respect to the network size and canalyzation depth, which is viewed also as a fraction of the number of variables of the PNCFs. The results provide a further in-depth understanding of the long term effect of perturbations on a PNCF network.

4.1. **Dynamical Impact.** In this section we analyze $y_{k+1} = f(y_k)$ as defined in (3) in relation to the sensitivity of the network to small perturbations. More precisely, y_k is an indicator of the long-term damage spread of an initial perturbation, that is the *dynamical impact* of the initial perturbation after k iterations. On the other hand, $f'(0)$ is an estimate for how an initial small perturbation spreads after one iteration. This is the analog of the so-called sensitivity of the PNCF which measures the number of ways that one flip of a node toggles the output of the PNCF [12, 13, 19, 21]. One single flip is the smallest change one can apply. By averaging these sensitivities over the nodes, we obtain the average sensitivity of the network.

We explore the dynamical impact over many networks, by varying n and d, and over all possible initial conditions y_0 given by (2) with $m = 1, 2, \ldots, n$. More precisely we consider the averages over the varied parameters n and d of the quantities

$$Q(n,d) = \frac{max_{\{k \leq T, y_0\}}\, y_k}{\langle y_k \rangle_{\{k \leq T, y_0\}}}$$

and

$$s(n,d) = f\prime(0) = 1 + \frac{n-d-2}{2^{d+1}}$$

where the notation $\langle X \rangle_Y$ stands for the average of the inside quantity X over the given varied parameters Y. We compute the maximum and average y_k over a number of iterations to time T, and over all possible initial conditions y_0 to get $Q(n,d)$. We plot $\langle Q(n,d) \rangle_{n,d}$ versus $\langle s(n,d) \rangle_{n,d}$ (grouped in a histogram), with a 10% standard deviation error bar. In Figure 5 the maximum network size considered is $n = 20$, with $d = 0, 1, \ldots, n$ representing all degrees of canalyzing depth. Observe that the maximum impact is significantly

larger than the average impact around the critical value $f'(0) = 1$, corresponding to the critical sensitivity, or the so-called edge-of-chaos, which separates ordered dynamics from chaotic dynamics. As the sensitivity increases, the graph drops quickly, so the maximum impact becomes comparable to the average impact, and this happens for a wide range of sensitivity values as n increases beyond what is shown in Figure 5. At the same time, as n increases the peak of the graph reaches higher values (graphs not shown, but similar to Figure 5). Thus we note that the dynamical impact varies significantly across various values of the average sensitivity of the network.

We note here that similar results have been observed in [22] for random Boolean networks. In [22] the dynamical impact is computed on initial perturbations of a single node and shown to be mostly decreasing as well, and to vary across nodes with diverse sensitivities. The maximal and average impacts approach equality rather fast as in our case, but the difference between the maximum and average impact is not as big as in our case. Thus, canalyzing yields more variation of the impact of perturbations. We point out that in [22] the averages are computed over initial conditions, individual node perturbations, and over the long-term behavior of the individual functions of the network; also the simulations are performed with actual networks, as opposed to a mathematical formula as in the present case.

We are also interested in the impact of the ratio d/n over the dynamical impact. In Figure 6 we plot $\langle Q(n,d)\rangle_{n,d}$ versus $\langle s(n,d)\rangle_{n,d}$ (grouped in a histogram) for fixed values of d/n as specified in the titles. In this case we have eliminated the 10% standard deviation error bar for a simpler plot. We notice the increase of the vertical scale as d/n increases, meaning that the maximum impact is significantly larger than the average impact for values of the average sensitivity close to the critical value $f'(0) = 1$. Notice also the reduced average sensitivity for large proportions d/n.

4.2. **Expected damage and percolation transition.** Let us explore further the map (3) in view of identifying *percolation limits*. These represent threshold values of the parameters that generate a transition of the expected damage y_k to zero, so that the initial perturbation does not scale up with, say, an increase in those parameters beyond

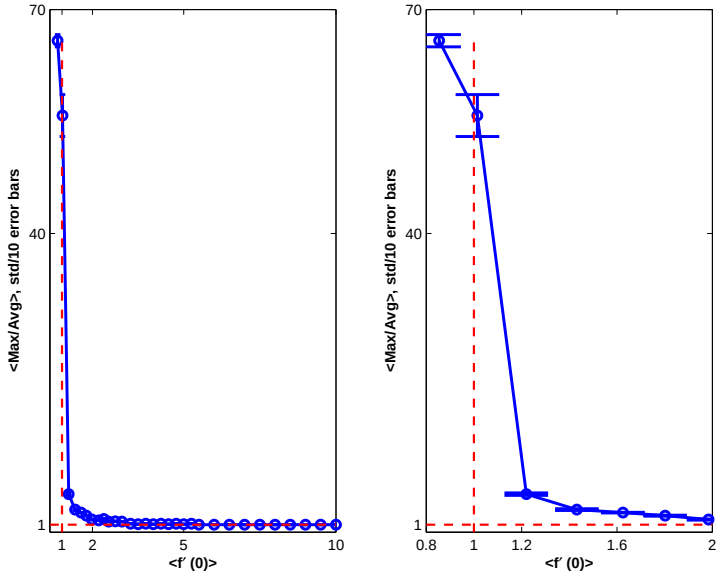

FIGURE 5. (Color online) Variation of the dynamical impact y_k across networks of sizes at most $n = 20$, with $d = 0, 1, \ldots, n$, ranging from no canalyzing through full canalyzation, and initial conditions y_0 given by (2). The averages are computed over $T = 200$ iterations. The horizontal axis represents the average sensitivities over all (n, d) combinations. We collect statistics of $Q(n, d)$ by values of $s(n, d)$ and plot the means with 10% error bars. Note that the maximum impact is much larger than the average impact for smaller sensitivity, but that they become roughly equal as $\langle f'(0)\rangle$ increases. The right graph is a zoom in on the left graph around the critical sensitivity $\langle f'(0)\rangle = 1$. The maximum impact is significantly larger than the average impact around the critical sensitivity $\langle f'(0)\rangle = 1$, followed by a clear drop leading to comparable values of the average and maximum impact for larger values of the average sensitivity. Thus the average sensitivity has a significant influence on the dynamical impact.

the threshold value. Percolation limits are explored for one parameter as some other parameters are allowed to vary. In particular it would be of interest to know if there are some "universal" percolation limits that do not depend on some of the parameters. For example, is it possible that there is a certain threshold of canalyzing depth above or below which the expected damage is reduced to zero regardless of the network size? A detailed explanation of percolation limits can be found in [23] for random Boolean networks where the average fraction of nodes that remain undamaged by an initial perturbation vanishes in the large system limit as the number of nodes increases without bound, or in [24] for finite random dynamical networks including random Boolean networks and threshold networks, with an approach that is further extended to small-world random Boolean networks in [25]. Although those papers are considering the percolation transition as the network size

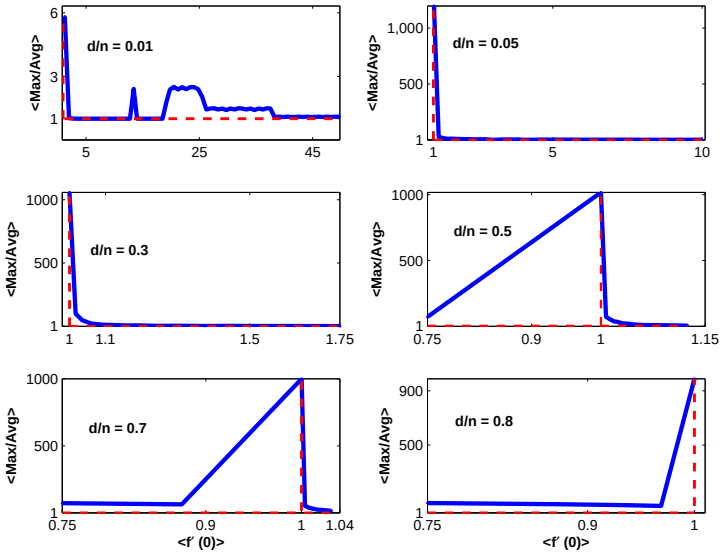

FIGURE 6. (Color online) Analog of Figure 5 with focus on the variation of the dynamical impact y_k across networks of sizes at most $n = 400$, with fixed ratios d/n as specified in the plots, ranging from reduced canalyzation through high canalyzation, and initial conditions y_0 given by (2). The horizontal axis represents the average sensitivities over all (n, d) combinations for each fixed ratio d/n. We collect statistics of $Q(n, d)$ by values of $s(n, d)$ and plot the means without the 10% error bars of Figure 5. Note that the maximum impact can be significantly larger than the average impact around $\langle f'(0)\rangle = 1$, but that they become roughly the same otherwise. Observe the change in the shape of the graphs as d/n increases, leading to mostly small values of $\langle f'(0)\rangle$ for increased level of canalyzation.

is increased, we will explore the transition to a null expected damage with respect to all the parameters under consideration.

For example, in the top plot of Figure 7 we plot $\langle y_{500}\rangle_{y_0}$ averaged over several values of the initial perturbation y_0 in the specified interval, versus the canalyzing depth d and various values of network size n within the bounds specified in the plot. The lowest curve for $n = 4$ and the highest one for $n = 4096$ generate an "envelope" for all the other curves with intermediate values of n. Any value larger than the maximal n generates a curve that is superimposed on the one for $n = 4096$, so an increase in network size does not provide any further insights. Notice that for large enough n, all graphs transition to zero around $d \sim 15$ regardless of the network size, so the (average) expected damage does not scale up with the network size. For smaller n values the graphs approach zero very fast. Thus, in terms of the canalyzing depth, the percolation limit appears to be around $d \sim 15$.

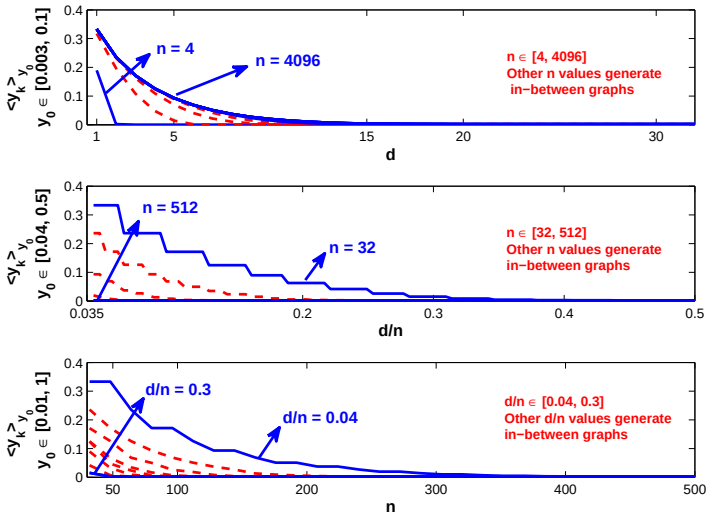

FIGURE 7. (Color online) Top: $\langle y_{500}\rangle_{y_0}$ averaged over several values of the initial perturbation y_0 in the specified interval, versus the canalyzing depth d and various values of the network size n within the bounds specified in the plot. For large enough n, all graphs transition to zero around the same value of $d \sim 15$, so the damage does not scale up with increased canalyzing depth. The graphs for $n > 4096$ are superimposed over $n = 4096$. Middle: Analog of the top figure, generated by replacing d with the ratio d/n which is independent of the network size. The (average) expected damage does not scale up with d/n. For canalyzing ratios $d/n > 0.35$ the expected damage is basically null for all n values, whereas for large enough values of n the transition to zero occurs for $d/n < 0.1$ with approximation. Bottom: Analog of the top figure, but with a switch of n and d/n. Notice that for $d/n \geq 0.3$ the transition to zero occurs for very small n values, approximately $n < 50$. Even for slightly larger values of d/n the damage still converges to zero for $n < 200$.

A somewhat similar situation is generated by replacing d with the ratio d/n which is independent of the network size. In this case the range of initial values y_0 can be extended as specified in the middle plot of Figure 7. The lowest and highest curve generate again an "envelope" for the intermediate values of n. Again, the (average) expected damage does not scale up with the network size and the transition to zero occurs for very small ratios d/n as n increases. Observe that the graph for the maximal n value is basically at zero altogether. The step-like graphs are natural as there are ranges of values of the ratio d/n that lead to the same outcome. Also, as n increases for a fixed d/n the values on the y-axis decrease. This is a reverse process than what was shown in the top plot of Figure

7. Notice that the percolation limit in terms of d/n is not as clear, but for large enough networks it is less than $d/n = 0.1$, which means a canalyzing depth of less than 10%.

Finally, we switch the roles of k and d/n in the previous figure and notice that for $d/n \geq 0.3$ the transition occurs for very small n values as seen in the bottom plot of Figure 7.

In conclusion, although there is no precise "universal" percolation limit, the transition to zero of the expected damage occurs for values in the neighborhood of some small values for $d, d/n$ or n, depending on the situation.

5. Discussion and Conclusions

We consider a network of PNCFs, that is, networks in which multiple inputs are canalyzing in a cascading fashion, while the remaining variables act according to a different type of Boolean rule. We track the effect/damage of an initial perturbation on the trajectories by finding a formula for the probability that a node's value is flipped by the initial perturbation after a number of time steps. Using that formula/model, (3), we show that the effect of perturbation decreases towards zero over time for PNCFs with canalyzation depth within two units from the number of inputs, and to a very small positive value otherwise. This is confirmed by generating approximations of the fixed points of the map (3) in formulas (8) and (9), and further exploring them, using Lyapunov exponents and bifurcation diagrams which indicate stability and convergence to zero of the perturbations. At the same time, the model is validated via simulations that match the model (3) with actual computations of Hamming distances under identical initial perturbations. We also explore the map (3) by regarding it as the dynamical impact of an initial perturbation after a number of iterations. By relating it to the average sensitivity of the network, which is the derivative of that map at zero, we show that the maximum dynamical impact of an initial perturbation after a number of iterations is comparable to the average impact for a wide range of sensitivity values; however around the critical value 1 for the average sensitivity, the maximum impact is significantly larger than the average impact; almost 70 times larger for networks of at most 20 nodes, and potentially hundreds of times larger for networks with a few hundreds of nodes regardless of the canalyzation depth. We finally

identify percolation limits, that is values of the parameters that generate a transition of the expected damage (generated by an initial perturbation) to zero as some parameters are increased, so that the initial perturbation does not scale up with the parameters once certain parameter thresholds are reached. We show that although there is not a clear "universal" percolation limit that does not depend on some of the parameters, such a transition occurs for sufficiently large networks, small canalyzing depths, or small connectivity values. More precisely, the transition to zero of the perturbations occur around a canalyzation depth of about 15 for sufficiently large networks, and in general for a ratio of the depth to the number of inputs that doesn't exceed 30%, but is typically less than 10%. The other way around, a network size of at least 200 nodes guarantees a transition to zero for any such ratio greater than about 10%.

There are several possible directions for future work. Regarding the actual model given by equation (3), one can generalize all the assumptions listed immediately after the equation, by assuming non-ergodicity, nonequal probability values for canalyzing or canalyzed states, as well as for the bias of the function g. Besides, not all nodes of the network need have the same canalyzing depth, follow the same order of canalyzation, or use the same function g. Moreover, assuming an extra level of perturbation such as asynchrony may provide a more plausible approach for most types of possible applications where intrinsic or environmental perturbations need to be taken into account.

Further extensions of this work could encompass heterogeneous networks in which PNCFs are combined with other types of Boolean functions, with varying connectivity, thus expanding the breadth of node types or Boolean functions that would contribute to the perturbations. For example, tracking perturbations on a probabilistic Boolean network where nodes can be governed by multiple rules that may be PNCFs or other types, would complement previous findings on those types of networks such as [26]. It would also be interesting to explore similar modeling for networks that are subject to feed-forward or feedback loops. This would introduce further correlations between the nodes that can build up as the network is evolved.

One can extend also the analysis of the percolation transitions, say with respect to the size of the initial damage, and consider how an initial damage scales with an increase in

parameters. Finally, this work can be extended to include repeated perturbations over time, following either a deterministic or a stochastic timing scheme, possibly coupled with varying sizes of perturbations (such as in medical treatments).

6. Acknowledgements

Part of the work of E.S.D. and O.I.Y. has been funded by the COST Action TD1210 KnowEscape.

References

[1] S. A. Kauffman, "Metabolic stability and epigenesis in randomly constructed genetic nets.," *J. Theor. Biol.*, vol. 22, no. 3, pp. 437–467, 1969.

[2] J. Saez-Rodriguez, L. Simeoni, J. Lindquist, R. Hemenway, U. Bommhardt, B. Arndt, U. Haus, R. Weismantel, E. Gilles, S. Klamt, and B. Schraven, "A logical model provides insights into T cell receptor signaling," *PLoS Comput. Biol.*, vol. 3, p. e163, 2007.

[3] A. Gambin, S. Lasota, and M. Rutkowski, "Analyzing stationary states of gene regulatory network using petri nets," *Silico Biology*, vol. 6, pp. 93–109, 2006.

[4] R. Albert and H. Othmer, "The topology of the regulatory interactions predicts the expression pattern of the segment polarity genes in *Drosophila melanogaster*," *J. Theor. Bio.*, vol. 223, pp. 1–18, 2003.

[5] F. Li, T. Long, Y. Lu, Q. Ouyang, and C. Tang, "The yeast cell-cycle network is robustly designed," *Proc. Natl. Acad. Sci.*, vol. 11, pp. 4781–4786, 2004.

[6] S. A. Kauffman, *The Origins of Order: Self-Organization and Selection in Evolution*. Oxford Universiy Press, 1993.

[7] C. H. Waddington, "Canalisation of development and the inheritance of acquired characters," *Nature*, vol. 150, pp. 563–564, 1942.

[8] F. Karlssona and M. Hörnquist, "Order or chaos in Boolean gene networks depends on the mean fraction of canalyzing functions," *Physica A*, vol. 384, pp. 747–757, 2007.

[9] S. A. Kauffman, C. Peterson, B. Samuelsson, and C. Troein, "Random Boolean network models and the yeast transcriptional network," *Proc. Natl. Acad. Sci.*, vol. 100, no. 25, pp. 14796–9, 2003.

[10] S. A. Kauffman, C. Peterson, B. Samuelsson, and C. Troein, "Genetic networks with canalyzing Boolean rules are always stable," *Proc. Natl. Acad. Sci.*, vol. 101, no. 49, pp. 17102–17107, 2004.

[11] S. Nikolajewa, M. Friedel, and T. Wilhelm, "Boolean networks with biologically relevant rules show ordered behavior.," *Biosystems*, 2006.

[12] L. Layne, E. Dimitrova, and M. Macauley, "Nested canalizing depth and network stability," *Bulletin of Mathematical Biology*, vol. 74, no. 2, pp. 422–433, 2012.

[13] K. Jansen and M. T. Matache, "Phase transition of boolean networks with partially nested canalizing functions," *Eur. Phys. J. B*, vol. 86, p. 86:316, 2013.

[14] C. Fretter, A. Szejka, and B. Drossel, "Perturbation propagation in random and evolved boolean networks," *New Journal of Physics*, vol. 11, p. 033005, 2009.

[15] T. Thimo Rohlf and S. Bornholdt, "Criticality in random threshold networks: annealed approximation and beyond," *Physica A*, vol. 310, p. 245259, 2002.

[16] J. Kesseli, P. Ramo, and O. Yli-Harja, "Tracking perturbations in boolean networks with spectral methods," *Physical Review E*, vol. 72, p. 026137, 2005.

[17] K. Ebadi, H. Klemm, "Boolean networks with veto functions," *Physical Review E*, vol. 90, p. 022815, 2014.

[18] A. S. Jarrah, B. Raposa, and R. Laubenbacher, "Nested canalyzing, unate cascade, and polynomial functions," *Physica D*, vol. 233, pp. 167–174, 2007.

[19] T. P. Peixoto, "The phase diagram of random boolean networks with nested canalizing functions," *Eur. Phys. J. B*, vol. 78, no. 2, pp. 187–192, 2010.

[20] L. Layne, *Properties and applications of nested and partially nested canalyzing functions*. PhD thesis, Clemson University, Clemson, SC, USA, 2011.

[21] I. Shmulevich and S. A. Kauffman, "Activities and sensitivities in Boolean network models," *Phys. Rev. Lett.*, vol. 93, no. 4, p. 048701, 2004.

[22] F. Ghanbarnejad and K. Klemm, "Impact of individual nodes in boolean network dynamics," *Europhysics Letters*, vol. 99, no. 5, p. 58006, 2012.

[23] B. Samuelsson and J. E. Socolar, "Exhaustive percolation on random networks," *Phys. Rev. E*, vol. 74, no. 3, p. 036113, 2006.

[24] T. Rohlf, N. Gulbahce, and C. Teuscher, "Damage spreading and criticality in finite dynamical networks," *Physical Review Letters*, vol. 99, p. 248701, 2007.

[25] Q. Lu and C. Teuscher, "Damage spreading in spatial and small-world random boolean networks," *Phys. Rev. E*, vol. 89, p. 022806, 2014.

[26] M. Brun, E. Dougherty, and I. Shmulevich, "Steady-state probabilities for attractors in probabilistic boolean networks," *Signal Processing*, vol. 85, pp. 1993–2013, 2005.